MAPPING THE AIR MOISTURE CHANGE IN UNDER CANOPY TREES USING A HEMISPHERICAL AND AERIAL PHOTOGRAPH BASED ON MACHINE LEARNING APPROACHES

Mochamad Firman Ghazali[1]
[1]Faculty of Engineering, Lampung University, Bandar Lampung, Indonesia
E-mail: firman.ghazali@eng.unila.ac.id

Received:15.12.2022; Revised:30.12.2022; Approved:31.12.2022

Abstract. The essential roles of trees in controlling the local climatic variation, such as air moisture, are still interesting to observe. Therefore, this study must deliver knowledge of the benefits of growing trees and enhance people's awareness of climate change adaptation. Here, the analysis requires several data fields such as hemispherical photography, an aerial photograph of a UAV, and air temperature collected using a wet and dry bulb thermometer, which has converted to air moisture. All these are considered to understand the air moisture change under the trees' canopy during a day observation. The hemispherical photography and aerial photograph of a UAV are processed to measure the tree's canopy size and then used together with interpolated air moisture to map the variation in air moisture distribution in under-canopy trees using random forest (RF) and Artificial Neural Network (ANN). The result shows that hemispherical photography describes the ability to control the air moisture change. As its size increases, the air moisture level tends to be higher. It was maintained at more than 70% compared to the area with lower canopy cover. This characteristic is similar to the pattern shown by the RF and ANN. However, the SVM has better results as it can separate air humidity in vegetated and non-vegetated areas.

Keywords: *hemispherical photography, trees canopy, air humidity, spatial distribution, aerial photograph*

1 INTRODUCTION

A discussion on micro-climate, sometimes known as the local climate, describes how the earth's surface conditions differ from those in the nearby surrounding areas. For instance, it is the climate in and around mountains, hills, rivers, lakes, coasts, forests, and cities (Yoshino, 2005). This situation appears as the result of the contribution of the bio-physical parameter that can indirectly control the amount of solar radiation beneath the earth's surface. As a result, It influences the variation of surface temperature. In this case, it also explains a relationship between the trees' ability to protect the earth's surface from loss of soil and air moisture caused by the penetration of solar radiation. A study by Pataki et al. (2021) provided evidence of tree support for local cooling, stormwater absorption, and health benefits of urban trees for residents.

A considerable effort has been made to map the local climate variation using various data products. Demuzere et al. (2022) used built-up vegetation cover, bare land, and water to map a 100m resolution global map of Local Climate Zones (LCZs). It computed a local climate and became the first model of local-global coverage for Local Climate Zones on the web (Demuzere et al., 2021). From these two studies, It is possible to learn the complexity of how local climates are formed. Therefore, As Aslam & Rana, (2022) said that numerous benefits of understanding the urban climate, air quality, and temperature at local levels might be achieved. Including crosscutting phenomena such as thermal comfort, urban planning, climate change adaptation, and energy use, as well as incorporating institutional and social aspects for climate change adaptation, urban resilience, and sustainability.

This article also offered methods for mapping the local climate variation. It specified only to observe the measured air temperature and estimated air humidity as controlled by the size of the tree's canopy. The tree's canopy plays the role of an umbrella which is blocked the solar light. It creates a difference in relative humidity between the upper leaves canopy can be much higher than under canopy (Lemmons, 2022), and it always occurs hourly temperature reductions (Shahidan, 2015). Along with the study conducted by Shahidan, (2015), it has been reported by Z. Huang et al. (2020) an empirical relationship between the impacts of tree canopy cover on microclimate. Both tree canopy cover and air temperature are linear correlated. It has a coefficient determination (R2) range from 0.6 to 0.89. From these explanations, It is possible to map the similar variation of measured air temperature and estimated air humidity in a local area. Additionally, the benefits of using remote sensing data like aerial photographs of UAVs and several hemispherical photographs believe in providing more reliable maps of both local climate variables.

2 RESEARCH METHODOLOGY

2.1 Study location

This study has taken place on the campus of Lampung University. This study site categorizes as an Af group of Koppen climate classification (Peel et al., 2007), So, Therefore, It has so many tropical trees planted that makes a composition between green open space (GoS) and built-up area at about 50%, recently (Figure 1). According to Maryanti et al., (2016), at least 30% of GoS should be available in an urban area. This means the campus of Lampung University has the potential to create local cooling and health benefits for all the people living there. To measure that potential, some of the campus policies should cope with the initiative to realize the sustainable development goals (SDGs), especially in goals 13 and 15 about Climate Action and Life on Land (United Nations, 2021)

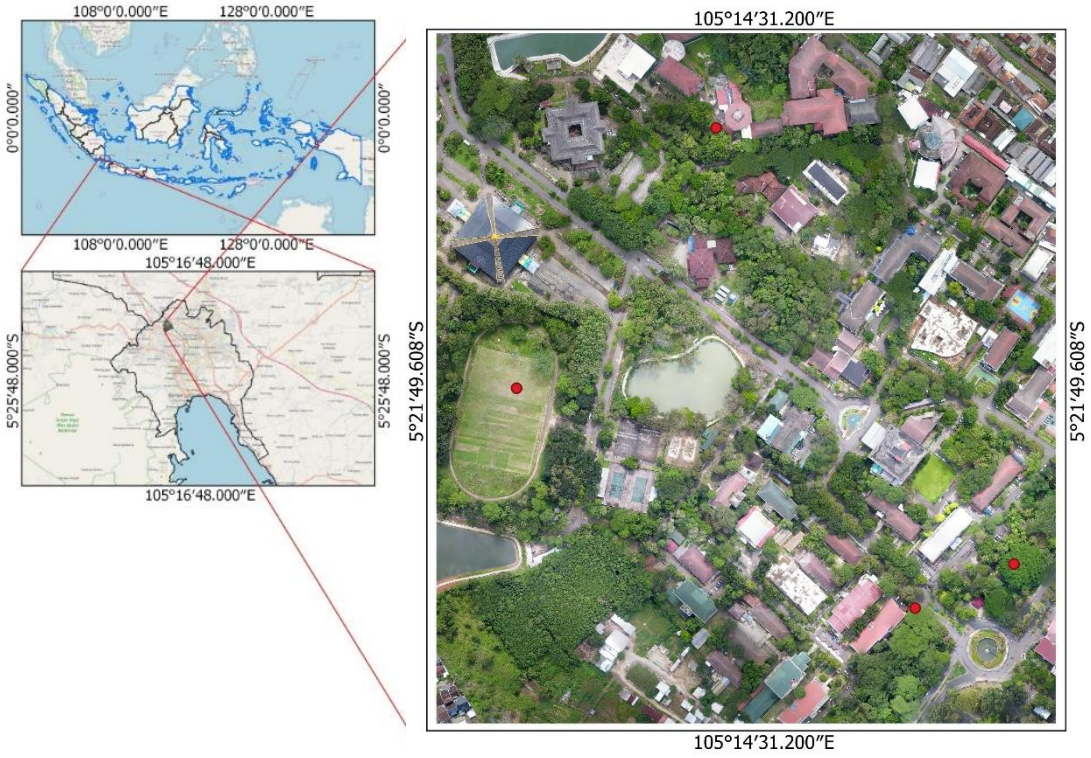

Figure 2-1. Study location for mapping the Air Moisture Change Under Canopy Trees. Red dots indicate the location samples used for observation.

2.2 Data and Its Processing

2.2.1 Air temperature

This study requires air temperature data to obtain the air moisture (air humidity), while its change can be achieved by looking for an empirical relationship between the air humidity, canopy trees, and land cover variation. The air temperature data were collected using a dry and wet bulb temperature during a day in drought season in 2021. As many as four locations were used to observe the variation in air temperature. These four locations have been chosen based on the trees' canopy characteristics, including the dense, moderate, lowest, and without canopy cover, but it is not bare soil. Besides that, the observation of air temperature started from 08.00 to 17.00. In the end, it successfully collected nine pairs of air temperature data from each location. Details of air temperature data can be shown in the table below (Table 1).

Table 2-1. Measured dry-wet bulb temperature (°C) on each locations

No	Latitude	Longitude	Dry bulb (°C)			The wet bulb (°C)		
			Min	Max	Average	Min	Max	Average
1	-5,36383	105,23995	27,5	30	26,5	25,5	28	26,5
2	-5,36168	105,24161	27	29,5	27,6	27	28,5	27,6
3	-5,36529	105,24407	27	30	27,4	26,5	28,5	27,4
4	-5,36566	105,24325	27	29,5	26,9	26,5	27,5	26,9

2.2.2 Air humidity and Its change

As explained by Huang et al., (2013), the air humidity can also be knowns by calculating the relative humidity (rH) using the dry and wet bulb equation (Eq. 1). This equation is made by following the principle of psychrometric hygrometry that require the saturated vapour pressure in the wet (e_w) and dry (e_d) bulb, coefficient humidity (A), mean atmospheric pressure (P), and the difference between the dry and wet bulb temperature (Δt).

$$rH = \left(\frac{e_w - A*P*\Delta t}{e_d}\right)x100 \quad (1)$$

$$\Delta t = T_d - T_w \quad (2)$$

$$e_w = 6.112 * 10^{\frac{17.502*T_w}{240.97+T_w}} \quad (3)$$

$$A = 0.00066 * (1 + 0.00115 * T_w) \quad (4)$$

The Δt should be computed using the formula (Eq. 2). The results will be used for the input for computing the rH. It will range from 1 to 10 depending on the air temperature value recorded by the dry bulb (T_d) and (T_w). Both e_w and e_d are possible to obtain using a multi-function, namely the Buck formula (Eq. 3). This formula can be easily modified by replacing the T_w by T_d When it uses to estimate the e_d. For A, an empirical formula proposed by Butler & García-Suárez, (2012), the P is equal to 1013.25024 mb. The entire computation process to obtain the rH using formula above (Eq. 1- 4) should be done carefully. Although, It can be also perform automatically using the relative humidity calculator provided on the internet at http://www.ringbell.co.uk/info/humid.htm or using the Mollier chart or Mollier diagram. This study also uses calculator assistance to compute the rH.

2.3 Interpolating estimated air humidity

In this process, estimated air humidity values are used for primary data input to retrieve their spatial distribution. An inverse distance weighted (IDW) was chosen to know the Spatio-temporal of how air humidity can be changed in larger areas. This process uses four sampling points, including nine estimated air humidity on each point, totally the IDW used thirty-six points. The consideration of using IDW is based

on much research on predicting the spatial distribution that mentioned the IDW (Jumaah et al., 2019; Kamboj et al., 2022; Nguyen et al., 2020). The formula for this process is available below (Eq.5-7). Where, w_i is the weight of the known point data x_i, d_{iz} is the Euclidean distance from the point data set, p is power, and Z is the result of interpolation (Razali & Wandi, 2019).

$$z = \frac{\sum_{i=1}^{n} w_i x_i}{\sum_{i=1}^{n} w_i} \quad (5)$$

$$w_i = \frac{1}{d_{ij}p} \quad (6)$$

$$d_{iz} = \sqrt{(x_i - x_z)^2 + (y_i - y_z)^2} \quad (7)$$

2.4 Hemispherical photography processing

This study used four hemispherical photos taken by a smartphone camera Nokia G20 equipped with a low-cost fish eye lens. These four hemispherical photos correspond to each location and physically describe the trees' canopy cover characteristics. However, quantitative information on how large the trees' canopy covered the earth's surface affected the air humidity is necessary to know. The relationship between the calculated canopy size and estimated air humidity corresponds to how the air humidity can be formed in nature. So, the known software of "can-eye", downloaded for free on the internet at https://www6.paca.inrae.fr/can-eye/Download, helped to extract the canopy size from these four hemispherical photos (Figure 2). Once the canopies' size is known, it might be possible to find their relationship to the change in air humidity.

2.5 Deriving a trees canopy cover based on the UAV green ratio to estimate the air humidity

The aerial photograph of UAVs of Dji Phantom V2.0 that flew at 08.00 am, from an altitude of 150 meters above the earth's surface, with 75% overlap, and required a flight duration of about 10'20" to complete the area of 2000 meters square. All the collected photos need to process into an orthophoto, and then after that, It can be used to measure the tree's canopy size based on its green ratio values, which can be computed using the formula proposed by Johansen et al., (2014) (Eq. 8).

$$Green\ ratio = \frac{G}{\left(\frac{R+G+B}{3}\right)} \quad (8)$$

(1) (2) (3) (4)

Figure 2-2. Hemispherical photos of four sampling locations at the soccer field (1), under the tree (2), Ficus benjamina (3), and mixed forest tropical trees (4) as the representation of unvegetated, lowest, moderate, and dense canopy cover, respectively.

The aim of using this green ratio is to measure the canopy cover size over the study area through linear regression. Where the y corresponds to the estimated trees canopy cover size in a raster format, a and b are regression coefficients, and the x are the pixel values of RGB images (Eq. 9). Studies have proven that the green ratio may closely relate to the tree's biophysical parameters. For instance, Harto et al., (2019) and Starý et al., (2020) used the same indices to detect the canopy area and distinguish the banana trees from

other vegetation types, while Beniaich et al., (2019) using the modified version of this formula for soil management and other studies preferred to used segmentation to analyze the canopy (Beniaich et al., 2019). In this study, using the green ratio is part of an experiment that can help complete the limit of canopy cover data.

$$y = ax + b \quad (9).$$

To map the air humidity, the random forest and artificial neural network algorithm will take this job. It requires a raster map of interpolated air humidity and estimated canopy cover at a specific observation time. This process is repeatable at all observation times. So, It can be assumed that the canopy cover size is stable over time, while the interpolated air humidity can be changed. Entirely it should be nine repetitions for random forest and ANN. Then, to compare both results, two average maps of air humidity resulting from the random forest and artificial neural network (ANN) must be compared to the average map of interpolated air humidity. Details of the entire process of this work shown in research flow below (Figure 2-3)

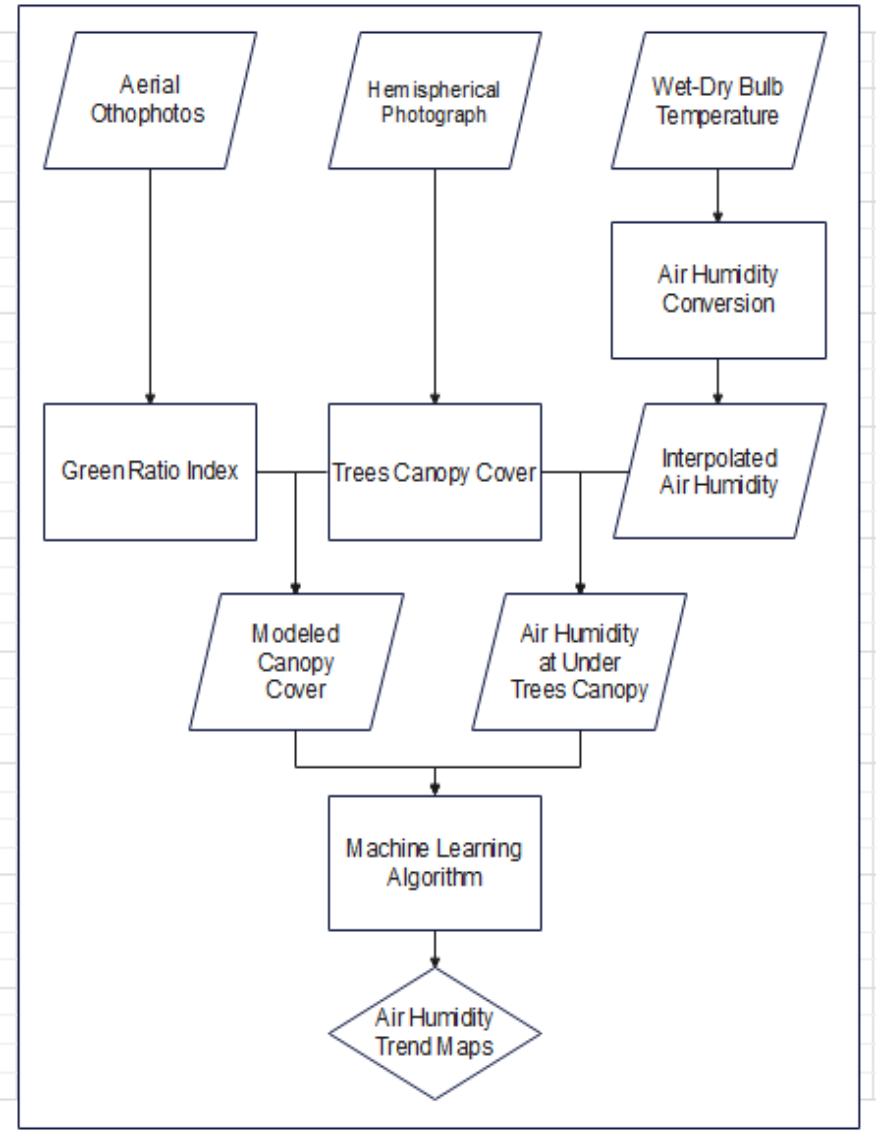

Figure 2-3. Research flow of air humidity mapping

3 RESULTS AND DISCUSSION

3.1.1 Temporal pattern of air temperature

Samples number 1 represents the bare soil area. It is similar to a soccer field located in the upper left corner of the study location (Figure 3-1). The air temperature was recorded at 27.5 OC in the morning and increased to 30 OC mid-day for a dry bulb. Different from samples 2, 3, and 4 correspond to the lowest, moderate, and dense canopy cover, respectively. It has the lowest temperature, 0.5 lower than sample number 1 in the morning, and rose to 29.5 OC, before decreasing to 28 OC at the end of the day. As representing the lowest and the dense trees canopy cover, samples 2 and 4, located under the (*Mimusops elengi* (Tanjung in bahasa) and mixed forest tropical trees, successfully gave the lowest air temperature during the day. However, sample number 3, situated near the *Ficus benjamina* (also named Beringin in Bahasa) has almost the same air temperature as sample number 1. The dry bulb thermometer shows the temperature at about 30 oC (Figure 3).

Especially for the wet bulb thermometer generally recorded the lowest air temperature compared to the dry bulb. The gap between dry and wet bulbs for samples 2, 3, and 4 ranges from -0.50 to 2, while 1 to 3.5 for sample 1. The important thing that can be learned from these data is that the higher difference between the air temperature values recorded by the wet and dry bulb thermometers will affect the air humidity value (Razak, 2007). In this case, the two land cover characteristics in the form of bare land will have a more significant difference when compared to those covered by vegetation (Ellison et al., 2017). Some parts of these graphs are also described by Colunga et al., (2015). Vegetation with high canopy cover had a lower temperature at 17:00 LT and higher at 9:00 to 10:00 LT during the warm season.

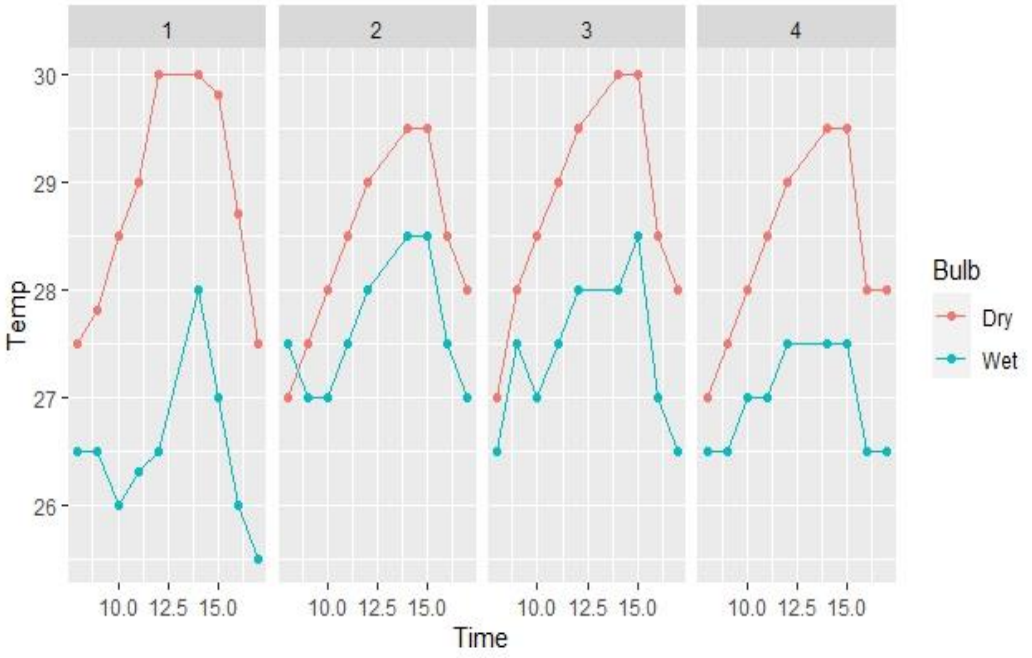

Figure 3-1. Temporal change of air temperature observed during a day observation in four trees canopy conditions using the dry-wet thermometer.

3.1.2 Temporal pattern of air humidity

The estimated rH will range from about 0 to 100%. These values show the amount of water that can be held in the atmosphere at a specific time. Here the rH range from 75.9 to 92% in location 1, 85.7 to 96.1% in locations 3 and 4, and 92 to 100 in location 2 (Figure 3-2). Consider using the graphs below. Learning the influence of a tree's canopy cover in determining air humidity is possible. The air humidity will be lower in the area without trees canopy cover than in the vegetated area. However, It may have different trees' canopy sizes, as visualized by graphs 2, 3, and 4, although they almost have a similar air humidity pattern. The air humidity pattern in numbers 1, 3, and 4 has its most profound point corresponding to their lowest air humidity level. It might have happened around 12.00 to 15.00. Unfortunately, this pattern does not appear in sample number 2.

3.1.3 Spatio-temporal of estimated air humidity

Since this study used minimal samples, and at the same time, the air humidity should be known entirely. The IDW helped a lot in estimating it. These nine maps expressed the Spatio-temporal of air humidity from 08.00 to 17.00. These maps are not only explaining the air humidity in under-canopy trees but also the surrounding. Generally, during the day, the lowest air humidity is located in the west or under the left part, while the highest air humidity is in the study area's upper or north part (Figure 3-3). Outside this pattern, three maps describe the peak (lower air humidity) describe the situation above that occurs in location 1 that may also influence the surrounding area.

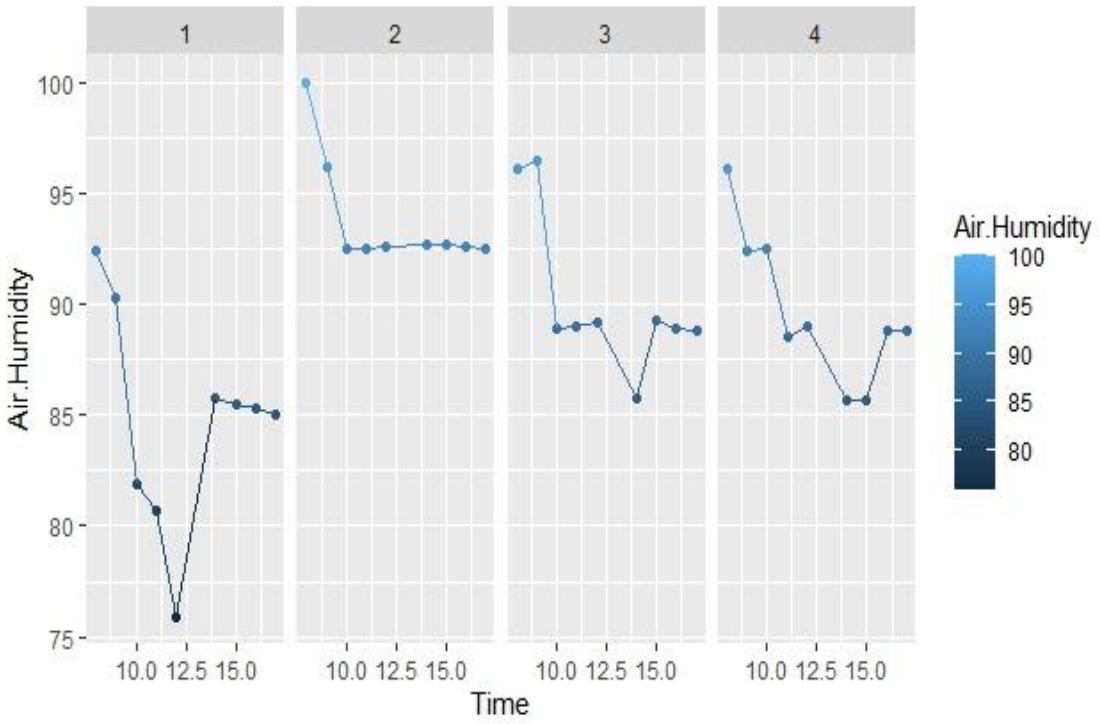

Figure 3-2. Temporal change of air moisture observed during a day observation in four trees' canopy conditions.

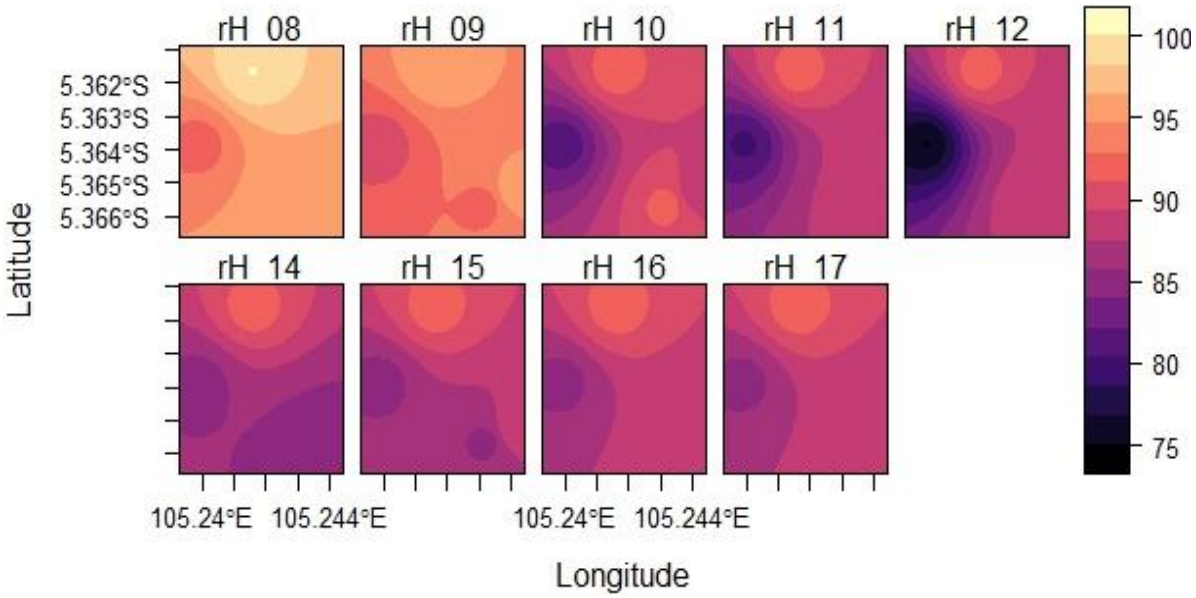

Figure 3-3. Spatio-temporal of estimated air humidity change during a day observation in four different tree canopy conditions.

A preliminary conclusion for this condition might be described in the soccer field, meadow land, and another type of land use without vegetation cover. Although the soccer field is also covered by grass, it differs from the air humidity over the trees. For other locations, the air humidity values also decrease after 12.00, even in the location covered by trees canopy. However, this spatial pattern was conducted in a limited time and coverage area. For that reason, additional effort is needed to know if this spatiotemporal can explain the same situation for a longer time and more extensive area. At least more observation is required to know the exact air humidity on a weekly or monthly basis. Besides that, it is critical to retrieve information on how air humidity differs along with the trees' canopy sizes.

3.1.4 Derived trees canopy from hemispherical photos, aerial photos of UAVs, and its relationship with air humidity

Analyzing four hemispherical photos for calculated canopy size using the cam_eye software resulted in a variation ranging from 18.48 to 64.5% (Table 2). These estimated tree's canopy cover relates to the change in the air humidity level during the day observation. According to the coefficient determination (R2), a situation before 12.00 shows values at about 0.42 to 0.74. It explains that the contribution of the tree's canopy cover has a moderate positive correlation with the increasing air humidity. However, this characteristic is slightly different after 12.00; the contribution of tree's canopy cover has become lower. It indicates the lower R2 at about -0.17 to 0.44 (Table 3). These two patterns are explicitly used to explain daily characteristics of air humidity change.

As mentioned before, the air humidity decreased from 08.00 to 12.00 and relatively increased from 15.00 to 17.00 (Figure 4). Sometimes, the canopy size has no rules to control these changes. If the canopy size increases, It successfully makes the local cooling several times, as Pataki et al., (2021) suggested. All these changes seem closely related to the amount of solar radiation that reaches the earth's surface instead of the canopy size. This situation is debatable since solar radiation is not involved as the experimental parameters. However, Tasie et al., (2018) have clearly explained this topic. In more extensive areas at the country level, the increase in relative air

humidity gives rise to a decrease in solar radiation and vice versa. It depicts an inverse relationship between humidity and solar radiation intensity. This statement is agreed with (Chatzithomas & Alexandris, 2015). Aside from this consideration, Tables 3-1 and 3-2 only explain the minor characteristics that are explicitly limited to the four sampling locations. For a more significant characteristic representing the larger area, the green ratio index map should be involved to map the canopy size in the entire study area.

Table 3-1. Processed trees canopy cover and estimated air humidity

No	Est. Tree's Canopy	Relative Humidity								
		08.00	09.00	10.00	11.00	12.00	14.00	15.00	16.00	17.00
1	18.48	92,4	90,3	81,9	80,7	75,9	85,8	85,5	85,3	85,0
2	40.19	100	96,2	92,5	92,5	92,6	92,7	92,7	92,6	92,5
3	64.5	96,1	96,5	88,9	89,0	89,2	85,8	89,3	88,9	88,8
4	57.33	96,1	92,4	92,5	88,5	89,0	85,7	85,7	88,8	88,8

Table 3-2. Correlation of estimated trees canopy cover to estimated air humidity

R2	08.00	09.00	10.00	11.00	12.00	14.00	15.00	16.00	17.00
	0,42	0,63	0,69	0,65	0,74	-0,17	0,19	0,42	0,44

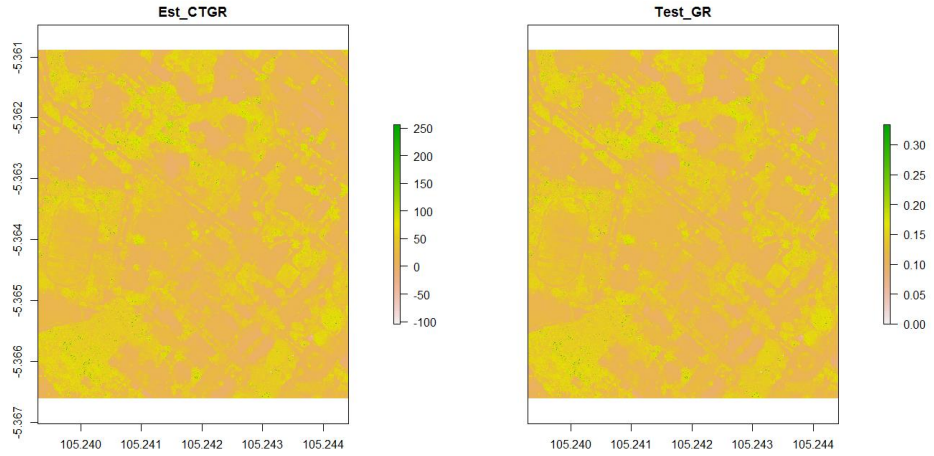

Figure 3-4. Estimated trees canopy cover (Est_CTGR) using the green ratio (Test_GR) based aerial photos of UAVs

An equation of $y = 1081.9x - 104.42$ with R2 = 0.7224 used to estimate a tree canopy cover map is formed based on the linear regression between y that represented estimated trees canopy cover and x as the green ratio map is helpful to provide a UAV based canopy cover map that ranges from 0 to 81.63 meters. 0 corresponds to the non-vegetated areas and mostly have a brown color, while the values more than 0 to 81.63 correspond to the vegetated area displayed by yellow to green colors (Est_CTGR). This configuration is also similar to the color used by Test_GR. The values below 0.10 correspond to non-vegetated areas, while more than 0.10 correspond with vegetated areas (Figure 3-4). Both values are highly positively correlated, with R2 equal to 1.

3.1.5 Spatio-temporal of estimated air humidity based on the machine learning algorithm

There are nine maps of air humidity under canopy trees estimated using the random forest algorithm, ANN, and Support Vector Machine (SVM) that correspond to the same time as the field

observation. For the random forest, It used ten maximum tree depths and two minimum sample counts, with 0.01 regression accuracy. For ANN, It used 0.1 as the weight gradient term and moment term, with sigmoid as the activation function of 1 alpha and beta functions, and the backpropagation as a training method and 3 for several layers and neurons. For SVM, It used C-SVC and radial basis function as SVM and Kernel type, with parameters of degree, gamma, coef0, C, nu-SVR, SVR Epsilon, cache size, and epsilon at 3, 0, 0, 1, 0.5, 0.1, 100, 0.001, respectively. All these machine learning algorithms ran in the SAGA GIS environment (Conrad et al., 2015).

Implementing the machine learning algorithm is challenging for air humidity estimation. It puts the result in a map facing difficulties when all the machine learning algorithms provide three different display styles. The advantage of using the SVM algorithm to map air humidity change from 08.00 to 17.00 in a day is that this method allows for separating air humidity based on the land cover type. It occurs without providing the landcover map before. It seems the algorithm knows their principal job is to map the air humidity under the canopy trees. In general, as displayed in maps rH_8, rH_9, rH_16, and rH_17, the lowest (0-0.5) air humidity correspond to the built-up objects, such as road, houses, and pool. Outside these objects, the vegetated areas are classified into two air humidity levels, moderate (0.5 – 1.5) and highest (1.5 – 3.0) (Figure 3-5a). However, the range values of low, moderate, and highest are not similar to interpolated air humidity map expressed by starting from 75 to 100 (Figure 3-4).

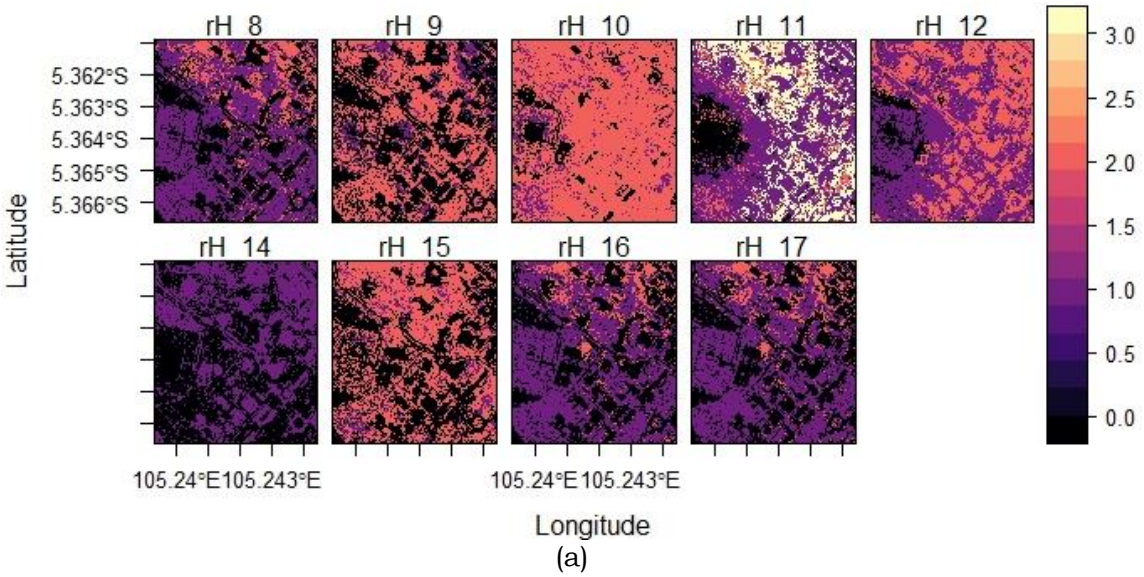

(a)

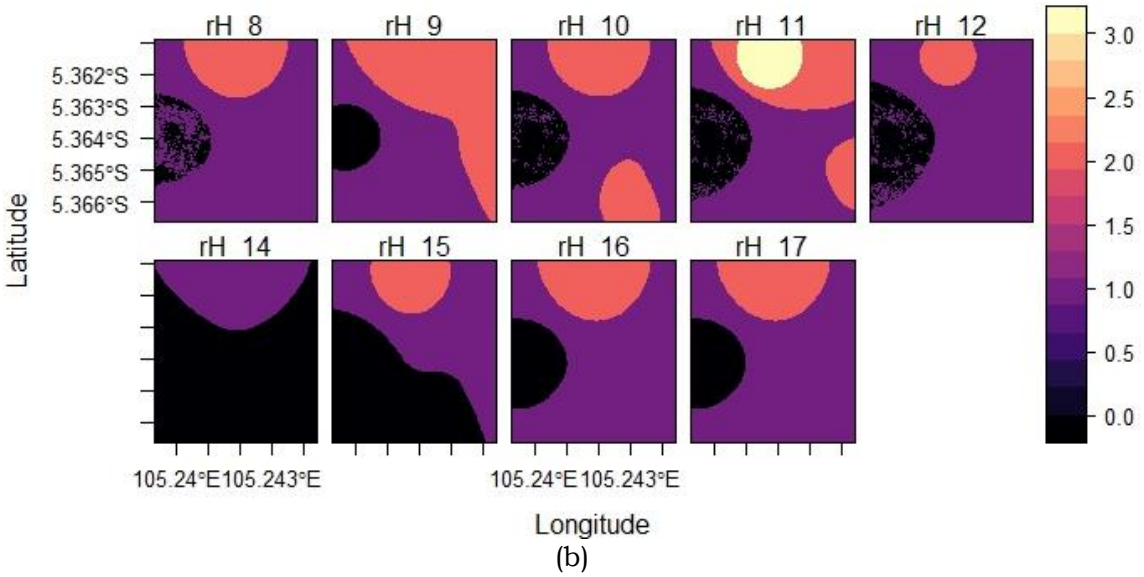

(b)

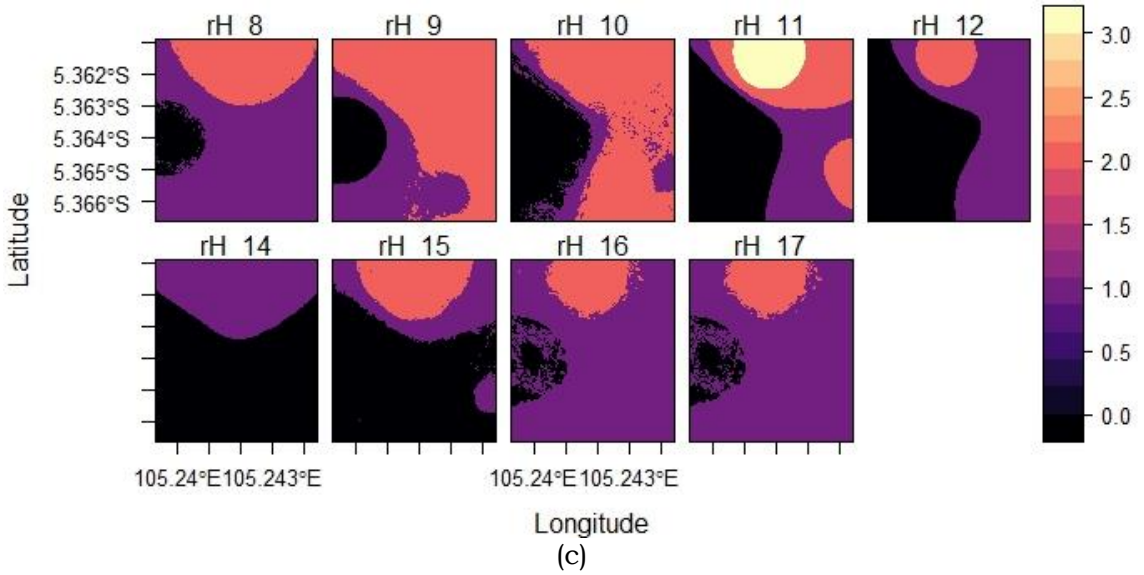

(c)

Figure 3-5. Spatio-temporal of estimated air humidity change during a day observation using SVM (a), RF (b), and ANN (c)

Unlike the interpolated maps of air humidity, the SVM shows the maximum air humidity that appears in rH_11. It is similar to the same maps produced by ANN and RF (Figures 3-5b and c). The RF allows the production of the maps in the same style as the interpolated maps and is grouped into two to three maps (Figure 3-5b). The display style of these maps is the same as the ANN (Figure 3-5c). Both maps produced through the ANN and RF cannot distinguish the air humidity in vegetated and non-vegetated areas. The result maps indicated the air humidity for the entire study location without differentiated objects on the surface. Even though these two predicted maps of ANN and RF also produced the same value range of air humidity with SVM.

The entire area of Lampung University, shown in Figure 3-1, has a vegetated area ratio equal to open green space at about 50%. This open green space effectively contributes to achieving moderate air humidity levels since all the predicted maps are generally given a similar situation. This situation also agreed with a study by Meili et al., (2021) that vegetation's role measured and positively controlled the thermal during the daytime. Since the thermal is close to air humidity, the higher vegetated ground fraction provides more cooling during the daytime. In case of the vegetation cover decrease someday, it is

also possible to influence the air humidity under the canopy. Each map shows a model in rH_8 at location 1. In this area, the air humidity was lower than in other locations with vegetation cover. This is because, Increasing the urban zone canopy cover by 50% would also reduce the urban heat island (UHI) by 2.05 ºC (Colunga et al., 2015). The situation at Lampung University is similar to that explained in other places in a non-tropical region, such as Mexico. Colunga et al., (2015) reported that the minimum temperature was similar between canopy cover levels. However, relative humidity was higher in high canopy cover plots. In conclusion, vegetation with higher canopy cover improved environmental conditions regarding relative humidity and regularization of extreme temperatures during the warm season.

4 CONCLUSIONS

This study has successfully predicted the Spatio-temporal of air humidity, including its changes over time according to the hourly basis of observation. Behind this successful story, these study offer choices of methods starting from implemented spatial interpolation of IDW and considering the machine learning algorithms, namely RF, ANN, and SVM. The IDW may help predict air humidity using singular data, while the machine learning algorithms are suitable for estimating air humidity using plural data. Although their accuracy is not yet measured, besides other limitations like inadequate sample size and many machine learning applications, this situation has not been recommended by many studies which utilized the machine learning algorithm. Therefore, a deep investigation into this topic should be enhanced to get more stable results.

REFERENCES

Aslam, A., & Rana, I. A. (2022). The use of local climate zones in the urban environment: A systematic review of data sources, methods, and themes. Urban Climate, 42, 101120. https://doi.org/10.1016/J.UCLIM.2022.101120

Beniaich, A., Silva, M. L. N., Avalos, F. A. P., De Menezes, M. D., & Cândido, B. M. (2019). Determination of vegetation cover index under different soil management systems of cover plants by using an unmanned aerial vehicle with an onboard digital photographic camera. Semina:Ciencias Agrarias, 40(1), 49–66. https://doi.org/10.5433/1679-0359.2019v40n1p49

Butler, C. J., & García-Suárez, A. M. (2012). Relative humidity at Armagh Observatory, 1838-2008. International Journal of Climatology, 32(5), 657–668. https://doi.org/10.1002/joc.2302

Chatzithomas, C. D., & Alexandris, S. G. (2015). Solar radiation and relative humidity based, empirical method, to estimate hourly reference evapotranspiration. Agricultural Water Management, 152, 188–197. https://doi.org/10.1016/J.AGWAT.2015.01.019

Colunga, M. L., Cambrón-Sandoval, V. H., Suzán-Azpiri, H., Guevara-Escobar, A., & Luna-Soria, H. (2015). The role of urban vegetation in temperature and heat island effects in Querétaro city, Mexico. Atmosfera, 28(3), 205–218. https://doi.org/10.20937/ATM.2015.28.03.05

Conrad, O., Bechtel, B., Bock, M., Dietrich, H., Fischer, E., Gerlitz, L., Wehberg, J., Wichmann, V., & Böhner, J. (2015). System for Automated Geoscientific Analyses (SAGA) v. 2.1.4. Geoscientific Model Development, 8(7), 1991–2007. https://doi.org/10.5194/gmd-8-1991-2015

Demuzere, M., Kittner, J., & Bechtel, B. (2021). LCZ Generator: A Web Application to Create Local Climate Zone Maps. Frontiers in Environmental Science, 9(April).

https://doi.org/10.3389/fenvs.2021.637455

Demuzere, M., Kittner, J., Martilli, A., Mills, G., Moede, C., Stewart, D., Vliet, J. Van, & Bechtel, B. (2022). A global map of Local Climate Zones to support earth system Modelling and Urban Scale Environmental Science. Earth System Science Data, 14(8), 1–57. https://doi.org/https://doi.org/10.5194/essd-14-3835-2022

Ellison, D., Morris, C. E., Locatelli, B., Sheil, D., Cohen, J., Murdiyarso, D., Gutierrez, V., Noordwijk, M. van, Creed, I. F., Pokorny, J., Gaveau, D., Spracklen, D. V., Tobella, A. B., Ilstedt, U., Teuling, A. J., Gebrehiwot, S. G., Sands, D. C., Muys, B., Verbist, B., … Sullivan, C. A. (2017). Trees, forests and water: Cool insights for a hot world. Global Environmental Change, 43, 51–61. https://doi.org/10.1016/j.gloenvcha.2017.01.002

Harto, A. B., Prastiwi, P. A. D., Ariadji, F. N., Suwardhi, D., Dwivany, F. M., Nuarsa, I. W., & Wikantika, K. (2019). Identification of banana plants from unmanned aerial vehicles (UAV) photos using object based image analysis (OBIA) method (a case study in Sayang Village, Jatinangor District, West Java). HAYATI Journal of Biosciences, 26(1), 7–14. https://doi.org/10.4308/hjb.26.1.7

Huang, Y., Zhang, K., Yang, S., & Jin, Y. (2013). A method to measure humidity based on dry-bulb and wet-bulb temperatures. Research Journal of Applied Sciences, Engineering and Technology, 6(16), 2984–2987. https://doi.org/10.19026/rjaset.6.3682

Huang, Z., Wu, C., Teng, M., & Lin, Y. (2020). Impacts of tree canopy cover on microclimate and human thermal comfort in a shallow street canyon in Wuhan, China. Atmosphere, 11(6), 18. https://doi.org/10.3390/atmos11060588

Johansen, K., Sohlbach, M., Sullivan, B., Stringer, S., Peasley, D., & Phinn, S. (2014). Mapping banana plants from high spatial resolution orthophotos to facilitate plant health assessment. Remote Sensing, 6(9), 8261–8286. https://doi.org/10.3390/rs6098261

Jumaah, H. J., Ameen, M. H., Kalantar, B., Rizeei, H. M., & Jumaah, S. J. (2019). Air quality index prediction using IDW geostatistical technique and OLS-based GIS technique in Kuala Lumpur, Malaysia. Geomatics, Natural Hazards and Risk, 10(1), 2185–2199. https://doi.org/10.1080/19475705.2019.1683084

Kamboj, K., Sisodiya, S., Mathur, A. K., Zare, A., & Verma, P. (2022). Assessment and Spatial Distribution Mapping of Criteria Pollutants. Water, Air, and Soil Pollution, 233(3). https://doi.org/10.1007/s11270-022-05522-y

Lemmons, R. (2022). Under the canopy. Climate Policy Watcher. https://www.climate-policy-watcher.org/vegetation/under-the-canopy.html

Maryanti, M. R., Khadijah, H., Uzair, A. M., & Ghazali, M. A. R. M. M. (2016). The urban green space provision using the standards approach: issues and challenges of its implementation in Malaysia. Sustainable Development and Planning VIII, 1, 369–379. https://doi.org/10.2495/sdp160311

Meili, N., Acero, J. A., Peleg, N., Manoli, G., Burlando, P., & Fatichi, S. (2021). Vegetation cover and plant-trait effects on outdoor thermal comfort in a tropical city. Building and Environment, 195(February), 107733. https://doi.org/10.1016/j.buildenv.2021.107733

Nguyen, T. Q., Nguyen, D. H., & Nguyen,

L. T. T. (2020). Personal air quality index prediction using inverse distance weighting method. CEUR Workshop Proceedings, 2882, 3–4.

Pataki, D. E., Alberti, M., Cadenasso, M. L., Felson, A. J., McDonnell, M. J., Pincetl, S., Pouyat, R. V., Setälä, H., & Whitlow, T. H. (2021). The Benefits and Limits of Urban Tree Planting for Environmental and Human Health. Frontiers in Ecology and Evolution, 9(April), 1–9. https://doi.org/10.3389/fevo.2021.603757

Peel, M. C., Finlayson, B. L., & Mcmahon, T. A. (2007). Updated world map of the Koppen-Geiger climate classification. Hydrology and Earth System Sciences, 11, 1633–1644. https://doi.org/10.5194/hess-11-1633-2007

Razak, A. M. Y. (2007). Power augmentation. In Industrial Gas Turbines. Woodhead Publishing. https://doi.org/10.1533/9781845693404.2.376

Razali, M., & Wandi, R. (2019). Inverse Distance Weight Spatial Interpolation for Topographic Surface 3D Modelling. TECHSI - Jurnal Teknik Informatika, 11(3), 385. https://doi.org/10.29103/techsi.v11i3.1934

Shahidan, M. (2015). Potential of Individual and Cluster Tree Cooling Effect Performances Through Tree Canopy Density Model Evaluation in Improving Urban Microclimate. Current World Environment, 10(2), 398–413. https://doi.org/10.12944/cwe.10.2.04

Starý, K., Jelínek, Z., Kumhálova, J., Chyba, J., & Balážová, K. (2020). Comparing RGB-based vegetation indices from uav imageries to estimate hops canopy area. Agronomy Research, 18(4), 2592–2601. https://doi.org/10.15159/AR.20.169

Tasie, N. N., Israel-Cookey, C., & Banyie, L. J. (2018). The Effect of Relative Humidity on the Solar Radiation Intensity in Port Harcourt, Nigeria. International Journal of Research, 5(21), 128–136. https://journals.pen2print.org/index.php/ijr/article/view/16369

United Nations. (2021). Goal 13 | Department of Economic and Social Affairs. Sustainable Development. https://sdgs.un.org/goals/goal13

Yoshino, M. (2005). Local Climatology. In J. E. Oliver (Ed.), Encyclopedia of World Climatology (pp. 460–467). Springer Netherlands. https://doi.org/10.1007/1-4020-3266-8_128